Role of Rab GDP dissociation inhibitor α in regulating plasticity of hippocampal neurotransmission

Hiroyoshi Ishizaki*, Jun Miyoshi*†, Haruyuki Kamiya‡§, Atsushi Togawa*, Miki Tanaka*†, Takuya Sasaki¶‖, Katsuaki Endo, Akira Mizoguchi††, Seiji Ozawa‡§, and Yoshimi Takai*¶‡‡**

*§§Takai Biotimer Project, Exploratory Research for Advanced Technology, Japan Science and Technology Corporation, c/o JCR Pharmaceuticals, Kobe 651-2241, Japan; ¶Department of Molecular Biology and Biochemistry, Osaka University Graduate School of Medicine/Faculty of Medicine, Osaka 565-0871, Japan; ‡Department of Physiology, Gunma University School of Medicine, Maebashi, Gunma 371-8511, Japan; §Core Research for Evolutional Science and Technology, Japan Science and Technology Corporation, Kawaguchi, Saitama 332-0012, Japan; **Department of Physiology, and ††Department of Anatomy and Neurobiology, Kyoto University Graduate School of Medicine/Faculty of Medicine, Kyoto 606-8501, Japan

Communicated by John A. Glomset, University of Washington, Seattle, WA, August 11, 2000 (received for review April 14, 2000)

Rab GDP dissociation inhibitor α (Rab GDIα) is a regulator of the Rab small G proteins implicated in neurotransmission, and mutations of Rab GDIα cause human X-linked mental retardation associated with epileptic seizures. In Rab GDIα-deficient mice, synaptic potentials in the CA1 region of the hippocampus displayed larger enhancement during repetitive stimulation, which was apparently opposite to the phenotype of Rab3A-deficient mice. Furthermore, the Rab GDIα-deficient mice showed hypersensitivity to bicuculline, an inducer of epileptic seizures. These results suggest that Rab GDIα plays a specialized role in Rab3A recycling to suppress hyperexcitability via modulation of presynaptic forms of plasticity.

Neurotransmitter release is a highly dynamic process involving the transport, docking, and fusion of vesicles at the presynaptic membrane and plays critical roles in synaptic plasticity, generally defined as an altered electrical activity depending on the prior stimulation (1). The short-term plasticities include paired-pulse facilitation (PPF), posttetanic potentiation (PTP), and depression, and range in duration from tens of milliseconds to several minutes (2), whereas the long-term synaptic plasticity at excitatory synapses in the hippocampus is called long-term potentiation (LTP) and is believed to underlie learning and memory (3). Although many biochemical steps are involved in synaptic plasticity, Rab3A, a member of the Rab small G protein family, is a key molecule in modulating the levels of neurotransmitter release in neurons (4).

Studies on Rab3A-deficient mice in the CA1 of the hippocampus have revealed an important insight into Rab3A function (5–7). Synaptic depression is increased after short trains of repetitive stimuli (5). Although CA1 LTP and two forms of short-term synaptic plasticity, PPF and PTP, are unaffected (5), mossy fiber LTP in the CA3 region is abolished (6). Because a more-than-usual number of exocytic events occur within a brief time after arrival of the nerve impulse (7), Rab3A is suggested to play roles in either recruitment of synaptic vesicles or, more likely, Ca^{2+}-triggered membrane fusion.

To understand the precise mechanism of Rab3A function, interactions with regulator proteins such as Rab GDP dissociation inhibitor (GDI) are likely to be important. Rab GDI is a general regulator of all of the Rab small G proteins that are implicated in intracellular vesicle trafficking (4, 8–10). Mammalian Rab GDI consists of three members: Rab GDIα, -β, and -γ, and Rab GDIα is specifically expressed in neuronal tissue. Genetic analysis of X-linked nonspecific mental retardation (XLMR) has revealed that mutations of the Rab GDIα gene can cause this disease (11). It is of note that Rab GDIα is localized to the distal part of chromosome Xq28 (12), because genetic defects mapped in this region have recently been described to cause a syndromic form of XLMR that comprises epileptic seizures (13). These observations suggest that Rab GDIα has a specialized function of the neuronal cells that may be related to suppress hyperexcitability. It remains unknown, however, how the mutations of Rab GDIα cause prolonged epileptic seizures of XLMR through affecting Rab3A function.

To clarify the neuron-specific role of Rab GDIα, we have made here Rab GDIα-deficient mice and found that the main function of Rab GDIα is to suppress hyperexcitability by regulating presynaptic plasticity.

Methods

DNA Library Screening. The Rab GDIα cDNA was isolated from a mouse brain cDNA library λ TriplEx (CLONTECH) by using the bacterial strains and the manufacturer's protocol and sequenced by using Applied Biosystems DNA sequencer. A cDNA fragment encoding the N-terminal half region of Rab GDIα was subcloned into appropriate plasmid vectors and used as a probe for homology screening of 129SVJ mouse genomic library λ FIXII (Stratagene).

Generation of Rab GDIα-Deficient Mice. A targeting construct was made to replace 3′ half of the coding exon 2 and the following exons 3–6 with a neo-resistance gene cassette. RW4 embryonic stem (ES) cells were transfected and selected as described (14). Homologous recombination was verified by Southern hybridization using 5′ and 3′ external probes and the neo-resistance gene probe. Rab GDIα-deficient ES cells were microinjected into E3.5 C57BL/6J blastocysts and transferred to MCH pseudopregnant foster mothers to generate chimeras that were mated with BDF1 mice for germline transmission. Mice with mutant alleles were also backcrossed with C57BL/6 mice. Genotyping was performed by Southern hybridization and PCR using primers in the neo gene (5′-GGGCGCCCGGTTCTTTTTGTC-3′ and 5′-GCCATGATGGATACTTTCTCG-3′) and in the replaced Rab GDIα gene (5′-GGCTTCTAGTGAGTATGAGTC-3′ and 5′-AAGCTGGTTGTATGTAATGTA-3′).

Western Blot Analysis. An anti-Rab GDIα antibody was raised against the C-terminal region of Rab GDIα, 365–447 amino acid residues, fused to the glutathione *S*-transferase protein. An

Abbreviations: PPF, paired-pulse facilitation; EPSC, excitatory postsynaptic current; GDI, GDP dissociation inhibitor; LTP, long-term potentiation; PTP, posttetanic potentiation; XLMR, X-linked nonspecific mental retardation; ES, embryonic stem; GABA, γ-aminobutyric acid; AP5, 2-amino-5-phosphovaleric acid; NMDA, *N*-methyl-D-aspartate.

†Present address: Department of Molecular Biology, Osaka Medical Center for Cancer and Cardiovascular Diseases, Osaka 537-8511, Japan.

‖Present address: Department of Biochemistry, The University of Tokushima School of Medicine, Tokushima 770-8503, Japan.

‡‡To whom reprint requests should be addressed. E-mail: ytakai@molbio.med.osaka-u.ac.jp.

§§Takai Biotimer Project was closed in September 1999.

The publication costs of this article were defrayed in part by page charge payment. This article must therefore be hereby marked "*advertisement*" in accordance with 18 U.S.C. §1734 solely to indicate this fact.

anti-Rab GDIβ antibody was raised against the synthetic peptide (LEDLYKRFKLPGQPPASC) specific to the Rab GDIβ isoform. Mouse brains were homogenized in a lysis buffer of 320 mM sucrose, 20 mM Tris·Cl (pH 7.5), 2 mM EDTA, and 10 mM PMSF. Fifty micrograms of proteins were separated by SDS/PAGE, transferred to Immobilon membrane (Millipore), and blocked for 1 h in TBS containing 5% BSA. After incubation with the antibodies for 1 h and then with peroxidase-conjugated secondary antibody for 1 h, the blots were developed with ECL (Amersham Pharmacia). Subcellular fractionation of the whole mouse brain was performed as described (15).

Electrophysiology. Transverse hippocampal slices (0.3- to 0.4-mm thick) were prepared from the wild-type and mutant mice (4–10 wk old). The composition of the external recording solution was: 127 mM NaCl, 1.5 mM KCl, 1.2 mM KH_2PO_4, 1.3 mM $MgSO_4$, 2.4 mM $CaCl_2$, 26 mM $NaHCO_3$, and 10 mM glucose. The solution was saturated with 95% O_2 and 5% CO_2. Electrical stimulation (test pulses at 0.1 Hz, 0.1 ms duration, $\approx$200 μA intensity) was delivered through a concentric bipolar electrode inserted into the stratum radiatum of the CA1 region. Extracellular field recording and whole-cell patch-clamp recording were performed at room temperature (24–26°C). For the whole-cell experiments, picrotoxin (100 μM) was added to block γ-aminobutyric acid (GABA)ergic inhibition. An incision was made between the CA1 and CA2 regions to block the propagation of burst activities from CA2/3 areas. Patch pipettes were filled with an internal solution (pH 7.2) containing: 150 mM cesium gluconate, 0.2 mM EGTA, 8 mM NaCl, 10 mM Hepes, 2 mM Mg^{2+} ATP, and 5 mM QX-314 (Sigma). Recordings were made with axopatch 1D amplifier (Axon Instruments, Foster City, CA). Signals were filtered at 2 kHz, digitized at 10 kHz, and analyzed with PCLAMP software (Axon Instruments). Amplitude of the excitatory postsynaptic currents (EPSCs) or the initial slope of the field excitatory postsynaptic potentials was measured, and the data are expressed as mean ± SEM as a percentage of baseline. In a separate set of experiments, field excitatory postsynaptic potentials at the mossy fiber-CA3 synapse were recorded as described (16). Statistical analysis was performed by using Student's t test, and $P < 0.05$ was accepted for statistical significance. All these experiments were carried out in a blind fashion.

Electroencephalogram. To record electroencephalograms, mouse littermates at 26 wk of age were injected with 0.2–0.4 ml of 25 mM bicuculline (100–200 mg/kg) i.p. for induction of status of epileptic seizures. A stainless steel electrode was placed over the parietal skull, and the reference electrode was fixed to the left ear. Statistical analysis was performed by using Student's t test, and $P < 0.05$ was accepted for statistical significance. All these experiments were carried out in a blind fashion.

Results

Generation of Rab GDIα-Deficient Mice. The mouse Rab GDIα gene consists of 10 coding exons spanning the 6.8-kb DNA region. Rab GDIα-deficient ES cells were generated by homologous recombination using a targeting vector designed to delete 2.3 kb of genomic DNA containing four exons (from exon 3 to exon 6) of the Rab GDIα gene (Fig. 1*a*). When the targeting construct was electroporated into RW4 ES cells, two G418-resistant colonies homozygous for the Rab GDIα gene were obtained, because the Rab GDIα gene is located in the X chromosome. The genotypes of the G418-resistant colonies were confirmed by Southern hybridization. These ES clones were used to generate chimeric mice and successfully contributed to germline transmission. Because all of the Rab GDIα heterozygotes were female, male chimeric mice and female Rab GDIα heterozygotes were intercrossed to produce homozygous mutant offspring (Fig. 1 *b* and *c*). Weak signals hybridized to the 3′ probe were visible at the wild-type level in lanes of homozygous DNAs, but they were not derived from the Rab GDIα gene locus because mice homozygous for the disrupted allele expressed no intact Rab GDIα protein (Fig. 1*d*). The Rab GDIα-deficient mice were viable and fertile, and showed no morphological abnormalities in their brains, indicating that Rab GDIα is not essential for neural development. Behavioral analysis in relation to XLMR is currently underway.

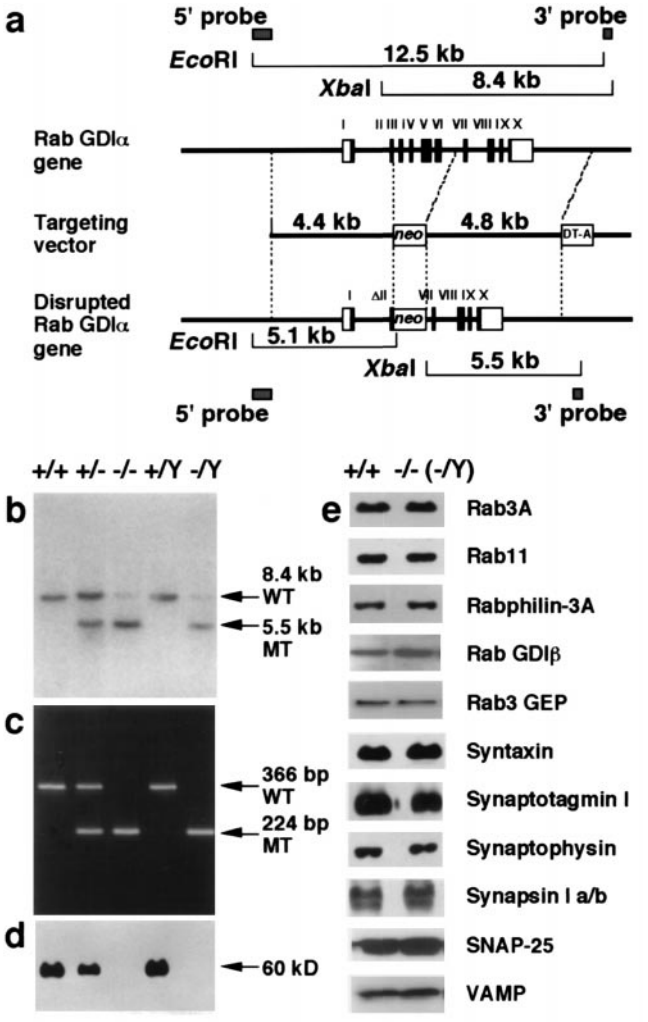

Fig. 1. Targeted disruption of the Rab GDIα gene. (*a*) Structure of the mouse Rab GDIα gene with 10 coding exons is shown at the top. A targeting vector was designed to remove part of the exon 2 and the following exons 3 to 6. The construct contained 4.4-kb 5′ flanking sequences and 4.8-kb 3′ flanking sequences. The MC1-neo cassette was inserted at the *Sac*I site within the exon 2, but the 5′ splice acceptor site was kept intact. The diphtheria toxin DT-A cassette was inserted at the 3′ end. In the targeted allele, the MC1-neo cassette replaces 2.4 kb of the genomic DNA region. Homologous recombination was verified by using informative restriction fragments and diagnostic probes as indicated. (*b*) Southern hybridization using *Xba*I-digested DNA extracted from mouse tails and the 3′ external probe shown in *a*. Mouse genotype was identified by the 8.4-kb wild-type (WT) and the 5.5-kb mutant (MT) fragments. (*c*) Genotyping by PCR analysis of DNA extracted from littermate mice at 21 days of age. PCR primers were selected to generate a 366-bp DNA product indicative of the WT allele or a 224-bp product because of the targeted (MT) Rab GDIα allele. (*d*) Western blot analysis of proteins extracted from the brain of each genotype. The 60-kDa band of the Rab GDIα protein was detected. (*e*) Western blot analysis of synaptic proteins extracted from the brain of the wild-type and Rab GDIα-deficient mice.

Steady-State Levels and Subcellular Localization of Rab3A and Relevant Proteins. Based on biochemical studies of Rab GDIα on Rab3A recycling, protein levels and subcellular localization of Rab3A and relevant proteins are expected to change in the Rab GDIα-deficient mice. In a previous report on the Rab3A-deficient mice, the rabphilin-3 level was selectively decreased to nearly 30% of that of the wild-type mice (5). It seems also likely that the protein level of Rab GDIβ increases to compensate Rab GDIα-deficiency. The Rab GDIα-deficient mice, however, showed normal steady-state levels of synaptic proteins, including Rab3A, Rab11, rabphilin-3A, Rab GDIβ, Rab3 GEP, syntaxin, synaptotagmin I, synaptophysin, synapsin I a/b, SNAP-25, and VAMP (Fig. 1*e*). The protein level of Rab GDIβ was unchanged in the extracts from the dissected parts, including the hippocampus (data not shown). The amounts of Rab GDIα were about 5-fold more than those of Rab GDIβ in the extracts from both the whole brain and the dissected parts (data not shown). We further examined subcellular localization of Rab3A by biochemical subcellular fractionation analysis, but did not detect significant differences in the distribution of Rab3A between the wild-type and Rab GDIα-deficient mice (data not shown). These results might be explained by rapid turnover of Rab3A activity, although it has not currently been shown that the cycling of Rab3A is the rate-limiting step in presynaptic neurotransmitter release.

Altered Plasticity of Hippocampal Neurotransmission in the Rab GDIα-Deficient Mice. To explore the physiological function of Rab GDIα in regulating synaptic transmission in the central nervous system, we examined whether the deletion of Rab GDIα changed synaptic transmission as well as several forms of activity-dependent plasticity at the excitatory synapses in the CA1 region of the hippocampus. It has already been demonstrated that the deletion of Rab3A in the nerve terminals results in accelerated synaptic depression during repetitive stimulation in the CA1 region (5). Therefore, we examined changes in this form of presynaptic plasticity. Repetitive stimulation at a moderate frequency (14 Hz) in the wild-type mice elicited an initial facilitation followed by a decrement of magnitude (Fig. 2*a*, upper trace). In contrast, the mutant synapse displayed a large accumulated facilitation during the train (Fig. 2*a*, bottom trace). The amplitudes of EPSCs elicited by 40 stimuli at 14 Hz in both the wild-type and mutant mice were summarized (Fig. 2*b*). The relative EPSC amplitudes at the end of train were 148 $\pm$ 13% (n = 13) and 207 $\pm$ 23% (n = 16) of the first EPSCs in the wild-type and mutant mice, respectively. The differences between the two groups were significant at the time points shown by asterisks ($P < 0.05$, Student's t test) (Fig. 2*b*). This phenotype of the Rab GDIα-deficient mice is apparently opposite to that of the Rab3A-deficient mice (5), suggesting that the proposed function of Rab3A, i.e., the recruitment of synaptic vesicles for exocytosis during repetitive stimulation, is enhanced in the Rab GDIα-deficient mice.

In the case of the Rab3A-deficient mice, the amplitude of successive EPSCs is virtually identical between the wild-type and mutant mice for the first 12 stimuli (5), indicating that Rab3A supports vesicle recruitment only after the 13th stimulus. In contrast, the differences were significant even from the second stimulus in this study (Fig. 2*b*). This raised a possibility that the synaptic facilitation is also modified in the Rab GDIα-deficient mice. To test this possibility, we next examined PPF, another form of presynaptic plasticity. As expected from the result in Fig. 2*b*, the magnitude of PPF was greater in the Rab GDIα-deficient mice than in the wild-type mice (Fig. 3*a*). Ratios of the second to the first EPSC amplitudes at 50-ms interstimulus interval were 186 $\pm$ 6% (n = 17) and 216 $\pm$ 7% (n = 15) in the wild-type and mutant mice, respectively (Fig. 3*b*). The differences between the two groups were significant at 50-ms and 70-ms intervals (*, $P <$ 0.05, Student's t test). On the other hand, PPF at longer intervals (100 ms, 200 ms, and 300 ms) were not different between the two groups. Enhanced PPF is not associated with alteration in its time course, indicating that PPF is enhanced not simply by a larger build-up of Ca^{2+} ions, but by modification of intrinsic properties of synaptic vesicles in the absence of Rab GDIα. This result, together with the enhanced synaptic facilitation during repetitive stimulation, suggests that the underlying mechanism of this form of short-term plasticity might depend on the Rab3A-mediated synaptic vesicular transport in addition to presynaptic Ca^{2+} dynamics.

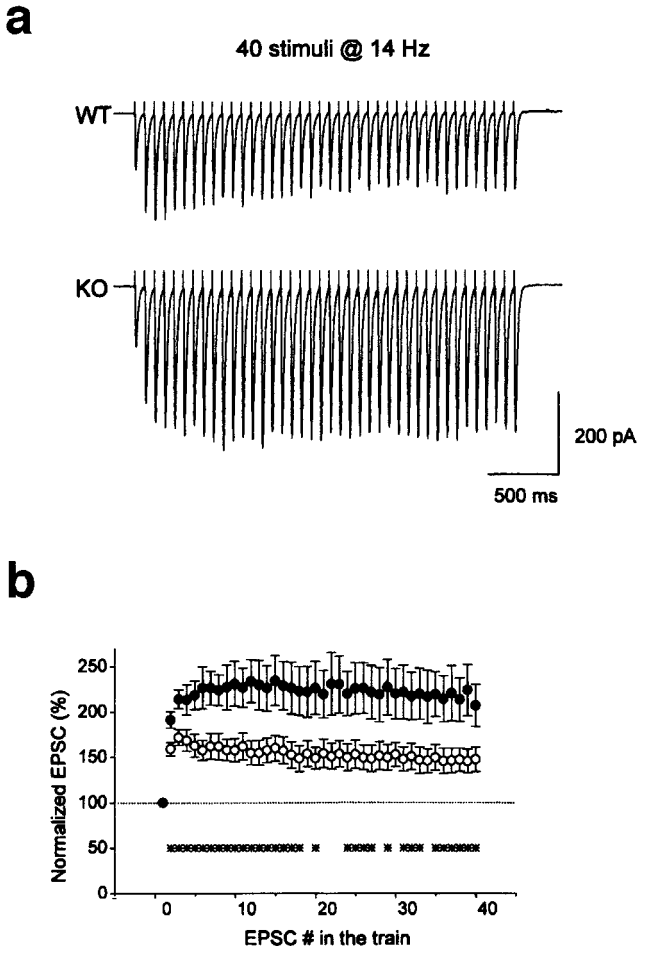

Fig. 2. Altered activity-dependent plasticity during repetitive stimulation in the Rab GDIα-deficient mice. (*a*) EPSCs in response to repetitive stimuli (40 stimuli at 14 Hz) of Schaffer collateral/commissural pathway were recorded from the CA1 neurons in slices from the wild-type (WT) and Rab GDIα-deficient mice (KO) in the presence of 50 μM D-2-amino-5-phosphovaleric acid (D-AP5). (*b*) Amplitudes of EPSCs plotted as a function of stimulus number during repetitive stimulation in the WT (○, n = 13) and mutant mice (KO, ●, n = 16). Amplitude of EPSCs was normalized to that of the first EPSC in the train. Ten trains of EPSCs were recorded every 30 s in each cell, and were averaged off-line. The differences between the two groups were significant at the time points shown by asterisks (*, $P < 0.05$, Student's t test).

Unaltered Rate of Blocking by MK-801 of Synaptic *N*-methyl-D-aspartate (NMDA) Response in the Rab GDIα-Deficient Mice. The magnitude of facilitation or depression depends on initial quantum content (2, 17). The changes in the basal release probability (P_r), therefore, might cause changes in short-term plasticity observed in the Rab GDIα-deficient mice. To examine whether P_r is altered in the mutant, we compared time courses of use-

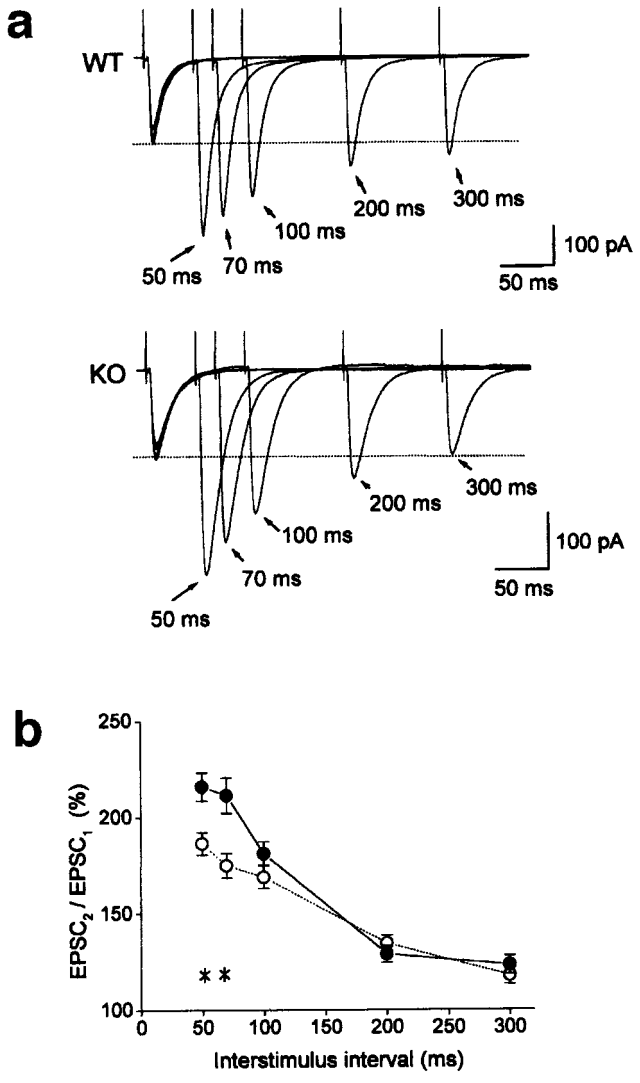

Fig. 3. Enhanced PPF in the Rab GDIα-deficient mice. (*a*) EPSCs recorded from the CA1 neurons of the wild-type (WT, top trace) and Rab GDIα-deficient mice (KO, bottom trace) in response to paired stimuli delivered to the Schaffer collateral/commissural pathway with different interstimulus intervals (50–300 ms) in the presence of 50 μM D-AP5. (*b*) Magnitude of PPF. Ratios of the second to the first EPSC amplitudes in WT (○, $n = 17$) and mutant mice (KO, ●, $n = 15$) are plotted as a function of interstimulus intervals. PPF at 50 ms and 70 ms were different between the two groups (*, $P < 0.05$, Student's t test).

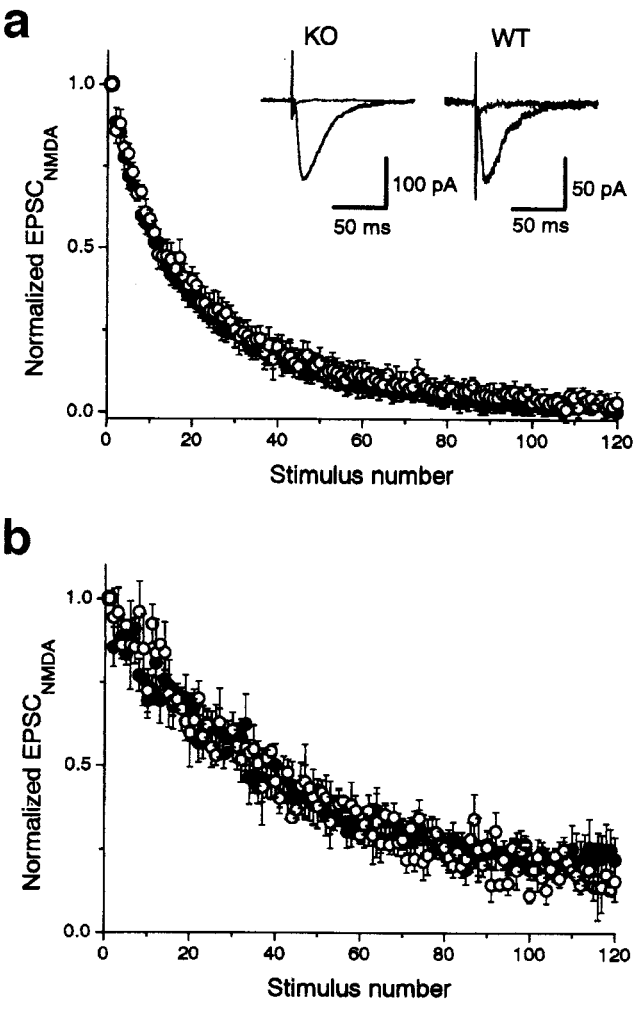

Fig. 4. Unaltered rate of blocking by MK-801 of NMDA receptor-mediated EPSC in the Rab GDIα-deficient mice. (*a*) Time course of the decrease of the amplitude of NMDA receptor-mediated EPSC ($EPSC_{NMDA}$) evoked every 10 s in the continuous presence of 40 μM MK-801, an open channel-blocker of NMDA receptor channels. $EPSC_{NMDA}$ was recorded at −40 mV in the presence of 10 μM 6-cyano-7-nitroquinoxaline-2,3-dione and 100 μM picrotoxin. The blocking rate of $EPSC_{NMDA}$ by MK-801 in the Rab GDIα-deficient mice (●, $n = 12$) was indistinguishable from that in the wild-type (○, $n = 11$). All values are normalized by the amplitude of the first EPSC recorded in the presence of MK-801. (*Insets*) Sample records in the slices of the wild-type (WT, *Right*) and mutant (KO, *Left*) mice, superimposing 1st and 120th responses. (*b*) Similar experiments in the presence of a low concentration (5 μM) of a competitive NMDA antagonist, D-AP5. The rate of blocking was slower under this conditions than in the absence of D-AP5, but again indistinguishable between the wild-type and mutant mice.

dependent blocking of NMDA receptor-mediated EPSC ($EPSC_{NMDA}$) in the presence of MK-801 (7, 18, 19), an irreversible open-channel blocker of the NMDA receptors (20), between the wild-type and mutant mice. In principle, an increase in P_r would result in a faster rate of progressive blocking of $EPSC_{NMDA}$. Time course of blocking of $EPSC_{NMDA}$ by MK-801 was not different between the two groups (Fig. 4*a*): the half decay time was 2.0 ± 0.2 min ($n = 11$) and 2.4 ± 0.3 min ($n = 12$) in the wild-type and mutant mice, respectively ($P > 0.33$, Student's t test). At least two exponentials, rather than single, are necessary to fit the decay time course of the progressive blocking of $EPSC_{NMDA}$ by MK-801 (18, 19). This fact might attribute to the presence of the two functionally distinct groups of synapses with low- and high-release probability (18). A selective increase in the population of low-release probability synapses, which, in turn, could result in changes in short-term plasticity, would not be readily detected by the measurement of half decay time, but could be resolved by the analysis of the late component of the decay. Therefore, we also fitted the time courses of $EPSC_{NMDA}$ blocking by MK-801 with the two exponentials, and the time constants and the fractions of the two components were compared between the wild-type and knockout mice. This analysis revealed no significant difference in the two groups (data not shown).

An increase in the number of vesicle released at a single release site would not change the rate of blocking by MK-801 under the normal conditions because of saturation of postsynaptic NMDA receptors by glutamate released from a single vesicle, and acceleration of the blocking rate would be detected only when a low concentration of D-AP5, a competitive antag-

onist of NMDA receptor, is added to the external solution. In fact, it has been reported that the blocking rate by MK-801 in the Rab3A-deficient mice is faster only in the presence of D-AP5 (7). However, the time course of MK-801 blocking was not different between the two groups: the half decay time was 6.0 ± 0.5 min ($n = 3$) and 5.6 ± 0.8 min ($n = 5$) in the wild-type and mutant mice, respectively ($P > 0.72$, Student's t test; Fig. 4*b*). These results suggest that basal release probability is not affected significantly by deletion of Rab GDIα, although we could not exclude completely the possibility that MK-801 test is not sensitive enough to detect a small change in basal neurotransmission.

Normal LTP in the CA1 and CA3 Regions in the Rab GDIα-Deficient Mice. We examined whether LTP in the CA1 region, an NMDA receptor-dependent form of synaptic plasticity, was altered in the Rab GDIα-deficient mice. LTP was essentially identical between the two groups: the wild-type, 148 ± 11% of baseline measured 60 min after induction ($n = 9$); the mutant, 155 ± 19% ($n = 7$; $P > 0.7$, Student's t test) (Fig. 5*a*). Because LTP in the CA1 region has been reported to be unaffected in the Rab3A-deficient mice (5), this form of long-term plasticity may be primarily independent of Rab3A function.

We also examined whether LTP at the mossy fiber-CA3 synapse is affected by the deletion of Rab GDIα, because LTP at this synapse is absent in the Rab3A-deficient mice (6). PTP or LTP was not different between the two groups (Fig. 5*b*). PTP (measured soon after tetanus) was 361 ± 25% ($n = 12$) and 393 ± 26% ($n = 12$) in the wild-type and mutant mice, respectively ($P > 0.41$, Student's t test). LTP (measured at 60 min after the tetanus) was 118 ± 4% and 120 ± 4% in the wild-type and mutant mice, respectively ($P > 0.67$). Thus, NMDA-independent synaptic plasticity at mossy fiber-CA3 synapse was unchanged in the Rab GDIα-deficient mice, suggesting that, although Rab3A is essential for mossy fiber LTP (6), its hyperactivation does not enhance the LTP.

Increased Susceptibility to Epileptic Seizures Induced by a GABA Antagonist. Rab GDIα function is required for the development of normal intelligence, but it might be linked to inhibition of epilepsy, because mutations of the Rab GDIα gene are likely to lead to syndromic XLMR associated with epileptic seizures (13). Thus, it is conceivable that changes in the firing properties of Rab GDIα-deficient neurons would make this hyperexcitable state vulnerable to epileptic seizures.

To address this question in our animal model, we challenged the Rab GDIα-deficient mice with a GABA antagonist, bicuculline, because a loss of hippocampal GABA-mediated inhibition underlies the neuronal hyperexcitability. Although bicuculline induced generalized seizures in the wild-type and Rab GDIα-deficient mice, the wild-type mice required a greater dose of bicuculline (5.3 ± 1.0 mg per mouse, $n = 10$) than did the mutant mice (3.7 ± 0.4 mg per mouse, $n = 10$; $P < 0.05$, Student's t test). This hyperexcitability observed in the Rab GDIα-deficient mice might be caused partly by deficits in Rab3A recycling. Thus, we conclude that quantal neurotransmitter release may be precisely tuned through proper Rab function for which Rab GDIα is essentially required.

Discussion

This study has revealed a specialized role for Rab GDIα in neurotransmitter release in mammals. Because two isoforms of Rab GDIs, Rab GDIα and -β, are expressed in the brain, Rab GDIβ apparently fulfills essential GDI functions in mice lacking Rab GDIα. Such basic functions are required for survival because yeasts expressing only one isoform of Rab GDI are inviable when the gene is deleted (4, 8–10). Therefore, Rab GDIα appears to play an additional role in neuronal cells.

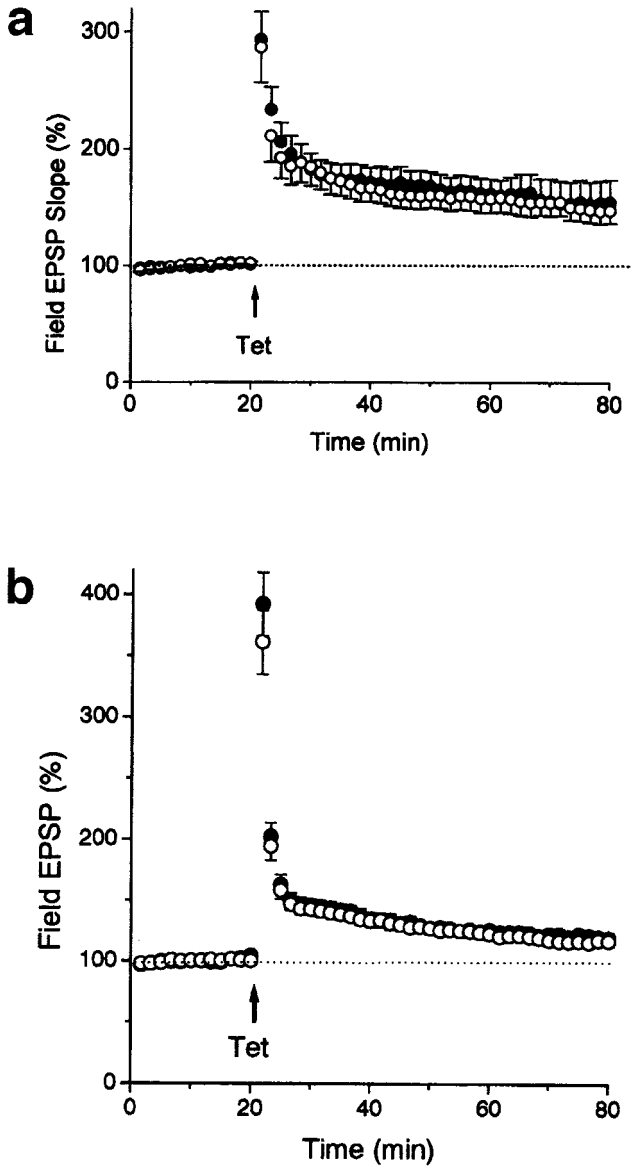

Fig. 5. Normal LTP in the Rab GDIα-deficient mice. (*a*) LTP at the Schaffer collateral/commissural-CA1 synapse in the wild-type and Rab GDIα-deficient mice. LTP was induced by two 1-s tetani at 100 Hz applied 20 s apart. There were no significant differences in LTP, measured at 60 min after the tetanus, between the wild-type (WT, ○, $n = 9$) and mutant mice (KO, ●, $n = 7$; $P > 0.7$, Student's t test). (*b*) LTP at the mossy fiber-CA3 synapse in the Rab GDIα-deficient mice. LTP was induced by 1-s tetani at 100 Hz in the presence of 25 μM D-AP5. There were no significant differences in LTP, measured at 60 min after the tetanus, between the WT (○, $n = 12$) and KO mice (●, $n = 12$; $P > 0.67$).

The phenotype of the Rab GDIα-deficient mice is apparently opposite to that of the Rab3A-deficient mice: Rab GDIα deficiency leads to a sharp increase in facilitation of excitatory transmission during repetitive stimulation, whereas Rab3A deficiency leads to a decrease under the same conditions (5). Such altered short-term synaptic plasticities are likely to culminate in hyperexcitability of the CA1 pyramidal neurons. The contrast, however, is not obvious in PPF and release probability: PPF is increased at short interpulse intervals (10–20 ms) in both cases, and no change in basal release probability is detected by MK-801 experiment in the Rab GDIα-deficient mice, but it is enhanced in the Rab3A-deficient mice (7). These results are not readily

explained by a role for Rab GDIα in suppression of the Rab3A recycling. It is possible that the normal Rab3A activity might already be saturated in the wild-type mice, although Rab3A exerts a suppressive action on basal release. Furthermore, it cannot be ruled out that the observed effects are also because of interference with the cycle of another Rab, e.g., Rab5, which has been shown to be expressed at a high level in synapses (21).

Biochemical studies have revealed three activities of GDI (4, 8–10): (*i*) GDI maintains a reserve, GDP-bound form of Rab in the cytosol; (*ii*) GDI transports this reserve pool to its respective target membranes where the GDP-bound form is converted to the GTP-bound form; and (*iii*) following conversion of the GTP-bound form to the GDP-bound form before, during, or after vesicle fusion, GDI retrieves Rab to the cytosolic reserve pool. Then, it is likely that a level of activated Rab3A is elevated on the synaptic vesicles and/or the presynaptic plasma membrane because of loss of Rab GDIα, if Rab GDIα functions in retrieving Rab3A from the membrane as well as in keeping them in the cytosol. Accumulation of activated Rab3A would lead to a more sensitive response to stimulation if the Rab3A cycle is the rate-limiting step. Although reduced Rab3A hinders docking efficiency in response to signals (7), enhanced Rab3A on the membranes may overstimulate the regulatory mechanism, thus leading to reduced accuracy of synaptic processes and elevated neurotransmitter release. Unfortunately, such an increase in the level of Rab3A has not been shown by conventional biochemical analysis.

Rab GDIα function is obviously required for the development of normal intelligence because Rab GDIα-deficiency leads to nonsyndromic XLMR (11). Moreover, Rab GDIα might be linked to inhibition of epileptic seizures because mutations in the distal part of chromosome Xq28 containing the Rab GDIα gene are likely to lead to syndromic XLMR that comprises anomalies of stature and epileptic seizures (13). In our animal model, the electrical activity associated with epileptic seizures was clearly detected in the Rab GDIα-deficient mice, which was more susceptible to bicuculline than the wild-type mice. This activity was probably recorded from the hippocampus because the hippocampus has the lowest seizure threshold in the brain (22). One of the underlying mechanisms must be attributed to enhanced synaptic facilitation during repetitive stimulation in the absence of Rab GDIα as observed in this study. Thus, we conclude that Rab GDIα has an important role *in vivo* to suppress hyperexcitability of the CA1 pyramidal neurons, and that changes in the firing properties of Rab GDIα-deficient neurons permit a breakthrough of this hyperexcitable state leading to epleptic seizures.

We thank Drs. Toshiya Manabe (Kobe University, Kobe, Japan) and William E. Balch (Scripps Research Institute, La Jolla, CA) for helpful discussions and critical reading of our manuscript. This investigation at Osaka University was supported by grants-in-aid for Scientific Research and for Cancer Research from the Japanese Ministry of Education, Science, Sports and Culture (1998 and 1999). Neurophysiological investigation at Gunma University was supported by grants-in-aid for Core Research for Engineering, Science, and Technology, Japan Science and Technology Corporation.

1. von Gersdorf, H. & Matthews, G. (1999) *Annu. Rev. Physiol.* **61,** 725–752.
2. Zucker, R. S. (1989) *Annu. Rev. Neurosci.* **12,** 13–31.
3. Bliss, T. V. P. & Collingridge, G. L. (1993) *Nature (London)* **361,** 31–39.
4. Takai, Y., Sasaki, T., Shirataki, H. & Nakanishi, H. (1996) *Genes Cells* **1,** 615–632.
5. Geppert, M. Bolshakov, V. Y., Siegelbaum, S. A., Takei, K., De Camilli, P., Hammer, R. E. & Sudhof, T. C. (1994) *Nature (London)* **369,** 493–497.
6. Castillo, P. E., Janz, R., Sudhof, T. C., Tzounopoulos, T., Malenka, R. C. & Nicoll, R. A. (1997) *Nature (London)* **388,** 590–593.
7. Geppert, M., Goda, Y., Stevens, C. F. & Südhof, T. C. (1997) *Nature (London)* **387,** 810–814.
8. Pfeffer, S. R., Dirac-Svejstrup, A. B. & Soldati, T. (1995) *J. Biol. Chem.* **270,** 17057–17059.
9. Wu, S-K., Zeng, K., Wilson, I. A. & Balch, W. E. (1996) *Trends Biochem. Sci.* **21,** 472–476.
10. Novick, P. & Zerial, M. (1997) *Curr. Opin. Cell Biol.* **4,** 496–504.
11. D'Adamo, P., Menegon, A., Lo Nigro, C., Grasso, M., Gulisano, M., Tamanini, F., Bienvenu, T., Gedeon, A. K., Oostra, B., Wu, S-K., *et al.* (1998) *Nat. Genet.* **19,** 134–139.
12. Sedlacek, Z., Konecki, D. S., Korn, B., Klauck, S. M. & Poustka, A. (1994) *Mamm. Genome* **5,** 633–639.
13. Armfield, K., Nelson, R., Lubs, H. A., Hane, B., Schroer, R. J., Arena, F., Schwartz, C. E. & Stevenson, R. E. (1999) *Am. J. Med. Genet.* **85,** 236–242.
14. Koera, K., Nakamura, K., Nakao, K., Miyoshi, J., Toyoshima, K., Hatta, T., Otani, H., Aiba, A. & Katsuki, M. (1997) *Oncogene* **15,** 1151–1159.
15. Fujita, Y., Shirataki, H., Sakisaka, T., Asakura, T., Ohya, T., Kotani, H., Yokoyama, S., Nishioka, H., Matsuura, Y., Mizoguchi, A., Scheller, R. H. & Takai Y. (1998) *Neuron* **20,** 905–915.
16. Kamiya, H. & Ozawa, S. (1999) *J. Physiol. (London)* **518,** 497–506.
17. Mallart, A. & Martin, A. R. (1968) *J. Physiol. (London)* **196,** 593–604.
18. Hessler, N. A., Shirke, A. M. & Malinow, R. (1993) *Nature (London)* **366,** 569–572.
19. Manabe, T. & Nicoll, R. A. (1994) *Science* **265,** 1888–1892.
20. Huettner, J. E. & Bean, B. P. (1988) *Proc. Natl. Acad. Sci. USA* **85,** 1307–1311.
21. Fischer von Mollard G., Stahl B., Walch-Solimena, C., Takei, K., Daniels, L., Khoklatchev, A., De Camilli, P., Südhof, T. C. & Jahn, R. (1994) *Eur. J. Cell Biol.* **65,** 319–326.
22. Traub, R. D., Miles, R. & Wong, R. K. S. (1989) *Science* **243,** 1319–1325.